General and Inorganic Chemistry

^{123}Sb NQR and ^{19}F NMR study of potassium, rubidium, and cesium heptafluorodiantimonates(III)

V. Ya. Kavun,[a]★ L. A. Zemnukhova,[a]★ V. I. Sergienko,[a] T. A. Kaidalova,[a] R. L. Davidovich,[a] and N. I. Sorokin[b]

[a]Institute of Chemistry, Far-Eastern Branch of the Russian Academy of Sciences, 159 prosp. 100-letiya Vladivostoka, 690022 Vladivostok, Russian Federation. Fax: +7 (423 2) 31 1889. E-mail: chemi@online.ru
[b]Institute of Crystallography, Russian Academy of Sciences, 59 Leninsky prosp., 119991 Moscow, Russian Federation. E-mail: sorokin1@mail.ru

The dynamics of crystal lattices of potassium, rubidium, and cesium heptafluorodiantimonates(III) and specific features of internal rotations of the Sb_2F_7 fluoride groups in these compounds were studied using ^{123}Sb NQR in the temperature interval from 77 to 325 K and ^{19}F NMR in the temperature interval from 240 to 470 K in combination with X-ray diffraction and thermogravimetric analyses. The distinctions in the dynamic behavior of the fluoride ions with changing the size (polarizability) of outer-sphere cations are discussed. The structural phase transition in $CsSb_2F_7$ was revealed at 425—430 K accompanied by the appearance of a high ion conductivity ($\sigma \approx 1.3 \cdot 10^{-3}$ S cm^{-1} at 450 K). A second type phase change can exist at 220—270 K.

Key words: antimony(III); potassium, rubidium, and cesium heptafluorodiantimonate(III) complexes; ^{123}Sb NQR spectroscopy, ^{19}F NMR spectroscopy, internal mobility, phase transitions.

Trivalent antimony fluoride complexes represent an extensive class of inorganic compounds, among which many substances exhibit unusual electrophysical,[1—3] optical,[4] and other properties, which stimulated their thorough investigation by different physicochemical methods.[1—3,5—13] In these compounds the influence of the nature of outer-sphere cations on the intensity of manifestation of these or other physical properties can clearly be traced, although the internal motions of the F^- ions and their relation to the size (polarizability) of the outer-sphere cations determining the structure of the MSb_2F_7 compounds were not virtually considered.

This work is a continuation of our studies of the antimony fluoride complexes[1,5,7,12—15] and is devoted to the ^{123}Sb NQR study of the dynamics of the crystal lattice of the MSb_2F_7 compounds (M = K, Rb, Cs) in the tempera-

Published in Russian in *Izvestiya Akademii Nauk. Seriya Khimicheskaya,* No. 11, pp. 1842—1848, November, 2002.
1066-5285/02/5111-1996 $27.00

ture interval from 77 to 325 K and the ^{19}F NMR study of the internal motions of the Sb_2F_7 fluoride groups in these compounds at 240—470 K.

Experimental

Polycrystalline compounds MSb_2F_7 (M = K, Rb, Cs) were synthesized using a previously described procedure.[13] The X-ray diffraction analysis of the samples was carried out on a DRON-2 diffractometer (Cu-Kα radiation). The thermal studies of the compounds were carried out using a Paulik-Paulik-Erdey derivatograph in the air with a rate of 5 deg min^{-1}. The weight of the samples was 600—800 mg.

Electrophysical characteristics of polycrystalline samples compacted in pellets were determined by the impedance method in the frequency interval from 5 to 500 kHz. A DAG-580 graphite paste was used for current-conducting contacts. The electroconductivity values σ were calculated from the active component of the complex resistance. The error of experimental data was 5%. The polarization of graphite electrodes (with the electronic type of conductivity) observed at low frequencies points to the ionic mechanism of electroconductivity in the compounds studied. Temperature studies were carried out in a vacuum of 0.1 Pa at 290—460 K using heating and cooling with thermostabilization at a series of fixed temperatures. The heating—cooling cycle was repeated at least two times for each sample.

^{123}Sb NQR spectra were recorded in the interval from 77 to 325 K on an ISSh-1-13 spectrometer with a temperature attachment (transitions with $\Delta m = \pm 1/2 \leftrightarrow 3/2$ (ν_1) and $\Delta m = \pm 3/2 \leftrightarrow \pm 5/2$ (ν_2) were studied). The accuracy of temperature measurements was ±0.3 K, and that of NQR frequency measurements was ±0.01 MHz. The quadrupole coupling constant (QCC) e^2Qq_{zz} and asymmetry parameter η of the tensor of the electric field gradient (EFG) were calculated from experimental NQR frequencies.[1,5,7] The accuracy of determination of QCC and η was ±0.1 MHz and ≤ ±0.1%, respectively.

^{19}F NMR spectra were recorded on a Bruker SWL 3-100 wide-line spectrometer (84.66 MHz) in the temperature interval from 240 to 470 K. The accuracy of temperature determination was ±1.5 K. The error of measurement of the second moments S_2 of NMR spectra did not exceed 5—8%, and the half-width of the resonance line ΔB was at most 2%. The structural data[8—10] were used in the calculation of the theoretical S_2 values using the van Vleck formula.[16] The activation energy E_a of internal motions in the fluorine sublattice was estimated using the equation $E_a = 154.7T_c$ (J mol^{-1}) and accepting the temperature of the beginning of decreasing S_2 or changing the resonance line shape (the appearance of a narrow signal in the NMR spectrum) as T_c.[16] The accuracy of estimation of E_a was ±1.5 kJ mol^{-1}. Chemical shifts (CS) δ (center of gravity of the NMR component or its components) were measured relatively to F_2 with an error of ≤3%.

Results and Discussion

The temperatures of polymorphous transformations and melting points of KSb_2F_7 (**1**), $RbSb_2F_7$ (**2**), and $CsSb_2F_7$ (**3**) are presented in Table 1. The structures

Table 1. Temperatures (K) of polymorphous transformation (T_{tr}) and melting points of the MSb_2F_7 compounds (M = K, Rb, Cs) in a helium flow[13] (I) and in the air (II)

Compound	T_{tr}		M.p.	
	I	II	I	II
KSb_2F_7 (**1**)	—	—	543	—
$RbSb_2F_7$ (**2**)	—	—	503	≥480
$CsSb_2F_7$ (**3**)	448	425	518	≥475

of the Sb_2F_7 dimeric groups in the heptafluorodiantimonates(III)[10] are shown in Fig. 3. Structure **3** contains[9] symmetric dimeric complex anions $[Sb_2F_7]^-$ formed by the combination of two SbF_3 molecules through the F bridging atom. The Sb atoms in structure **3** occupy the equivalent positions. In this compound, the trigonal bipyramid $SbEF_4$ (E is the lone electron pair of Sb^{3+}) is the coordination polyhedron of Sb. In structures **1** and **2**, the Sb atoms are in the nonequivalent positions. The KSb_2F_7 structure[8] consists of infinite chains formed by alternating $Sb(1)EF_3$ and $Sb(2)EF_4$ groups, which are connected by the asymmetric F(7) and F(2) bridges (see Fig. 1). The coordination polyhedra of Sb in $RbSb_2F_7$ are[10] trigonal bipyramids $Sb(1)EF_4$ and $Sb(2)EF_4$ sharing the F(5) atom to form layers. Thus, the structures of the MSb_2F_7 crystals have common features, but a change in the polarizability of the alkaline cation distorts the structural motive.[8—10,17] Such a distortion can affect the character of the dynamic behavior of the fluorine subsystem and central Sb atom when the external conditions change.

Analysis of ^{123}Sb NQR parameters. The ^{123}Sb NQR spectra of alkaline metal heptafluorodiantimonates(III) have previously been studied at 77 K.[5,7] The doublet structure of the spectra of compounds **1** and **2** agrees completely with the existence of two nonequivalent positions of the Sb atoms in the crystalline lattices of these com-

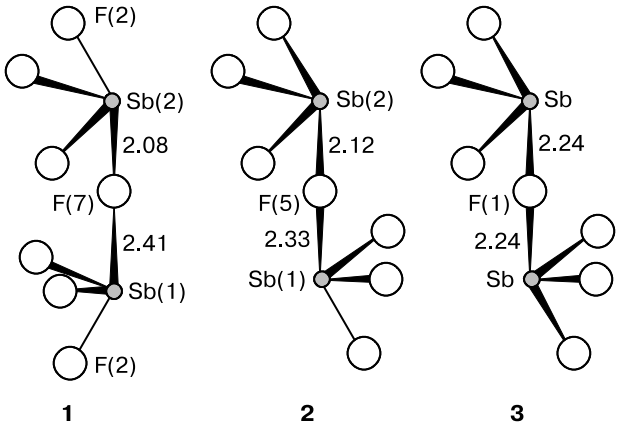

Fig. 1. Dimeric Sb_2F_7 groups in the MSb_2F_7 structures (M = K (**1**), Rb (**2**), and Cs (**3**)).[10] The interatomic F—Sb (Å) distances are presented.

pounds (see Fig. 1). The ^{123}Sb NQR frequencies for compound **1**, whose structure contains two distinct types of polyhedra, were assigned using the correlation of the asymmetry parameter of EFG to angular and structural distortions of the antimony polyhedra, according to which $\eta = 7.3\%$ characterizes the Sb(1) atoms in the $Sb(1)EF_3$ polyhedra (QCC = 702.6 MHz) and $\eta = 8.7\%$ characterizes the Sb(2) atoms in the $Sb(2)EF_4$ polyhedra (QCC = 674.1 MHz). The asymmetry parameters of the Sb(1) and Sb(2) atoms in the spectra of $RbSb_2F_7$ at 77 K are equal to 9.8 and 8.6%, and QCC are 672.5 and 694.9 MHz, respectively. The ^{123}Sb NQR spectrum of compound **3** exhibits, as should be expected, only one set of signals corresponding to the crystallographycally equivalent Sb atoms (QCC = 661.8 MHz). However, despite the high geometric symmetry of the anion in this compound, the asymmetry parameter of EFG on the Sb atoms are higher (at 77 K $\eta = 13.8\%$) than that for compounds **1** or **2**.

The doublet character of the ^{123}Sb NQR spectra for KSb_2F_7 indicates that the Sb(1) and Sb(2) atoms remain nonequivalent in the crystalline lattice at 77—298 K as well. In this compound, the NQR signals of the transition with $\Delta m = \pm 1/2 \leftrightarrow \pm 3/2$ (ν_1) decay at a lower temperature (230 K) than those for the transition with $\Delta m = \pm 3/2 \leftrightarrow \pm 5/2$ (ν_2). Therefore, the changes in the e^2Qq_{zz} and η parameters were calculated in the region from 77 to 230 K (Figs. 2 and 3). The QCC values for ^{123}Sb decrease with temperature (see Fig. 2, curves *1* and *2*), which agrees with the Bayer model.[18] This model takes into account that the EFG values are averaged due to libration vibrations of the crystalline lattice and the temperature coefficients of QCC and η take negative values. The calculated temperature coefficients of QCC ($\partial e^2Qq_{zz}/\partial T$) are equal to −115.7 (Sb(1)) and −143.0 (Sb(2)) kHz deg^{-1} and manifest no anomaly in the temperature interval studied. The temperature plots of the asymmetry parameters of EFG of the Sb(1) and Sb(2) atoms differ in the spectra of

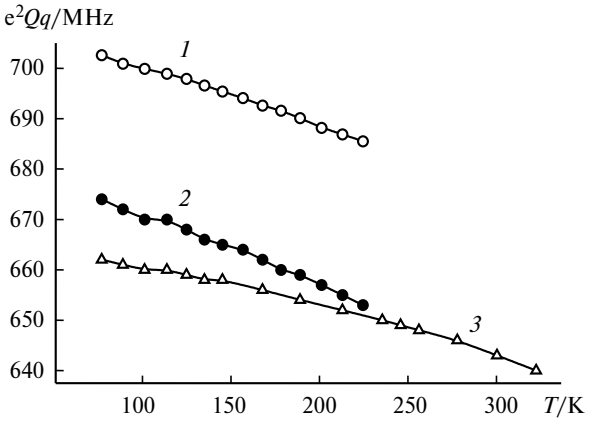

Fig. 2. Temperature plots of the quadrupole coupling constant (e^2Qq) of ^{123}Sb in KSb_2F_7 for Sb(1) (*1*) and Sb(2) (*2*), and in $CsSb_2F_7$ (*3*).

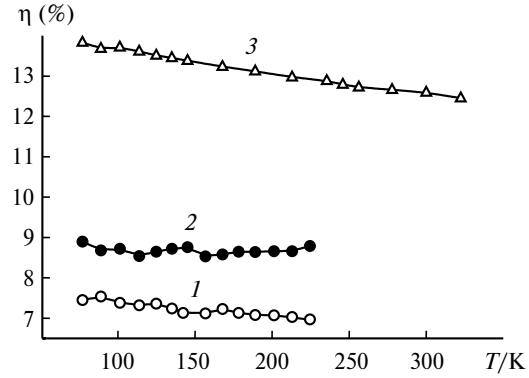

Fig. 3. Temperature plots of the asymmetry parameter of EFG (η) of ^{123}Sb in KSb_2F_7 for Sb(1) (*1*) and Sb(2) (*2*), and in $CsSb_2F_7$ (*3*).

compound **1** (see Fig. 3, curves *1* and *2*). For the Sb(1) atoms (see Fig. 3, curve *1*), the $\partial\eta/\partial$T coefficient equals $-3.3 \cdot 10^{-3}$ deg^{-1} in the whole studied temperature interval. This means that the symmetry of the EFG tensor in the region of localization of the quadrupole Sb(1) nucleus increases with temperature. The Sb(1) atoms at ~170 K exhibit a change in the sign and value of the $\partial\eta/\partial T$ temperature coefficient (see Fig. 3, curve *2*) from $-3.4 \cdot 10^{-3}$ deg^{-1} (77—170 K) to $+3.5 \cdot 10^{-3}$ deg^{-1} (170—230 K). The appearance of the positive sign at the $\partial\eta/\partial T$ temperature coefficient points to some symmetry decrease in the electron density distribution on the Sb(2) atoms with temperature.

The ^{123}Sb NQR spectra for compound **3** in the 77—322 K region consist of a single line for each transition, which indicates the single position of the Sb atom in the crystalline lattice. The temperature coefficients $\partial e^2Qq_{zz}/\partial T$ (−87.4 kHz deg^{-1}) and $\partial\eta/\partial T$ ($-5.6 \cdot 10^{-3}$ deg^{-1}) have standard "Bayer" negative values (see Figs. 2 and 3, curves *3*). However, in the 220—270 K region crystals **3** manifest weak piezoelectric properties observed from the appearance of characteristic piezoelectric noise in the radio-frequency field. The temperature interval, in which the piezoelectric phase exists, correlates with changes in the $\partial e^2Qq_{zz}/\partial T$ values from −71.6 (77—220 K) to −118.4 kHz deg^{-1} (270—322 K) and, correspondingly, $\partial\eta/\partial T$ (from $-6.0 \cdot 10^{-3}$ to -4.7–10^{-3} deg^{-1}). All these facts do not contradict the assumption about the second type of phase change.

Analysis of ^{19}F NMR spectra. The temperature plots of the second moments S_2 of the ^{19}F NMR spectra for compounds **1**—**3** and some characteristic spectra for these compounds reflecting the dynamic state of the fluorine subsystem are presented in Figs. 4—6. Based on the assumption that the Sb_2F_7 dimers represent the main structural unit in the MSb_2F_7 crystals (see Fig. 1), we calculated the second moments of the ^{19}F NMR spectra for the "rigid" lattice, which turned out to be almost the same for

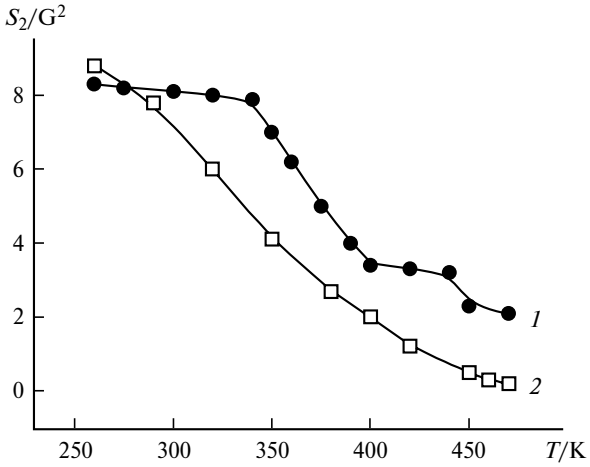

Fig. 4. Temperature plots of the second moment of the ^{19}F NMR spectra (S_2) for KSb_2F_7 (*1*) and $RbSb_2F_7$ (*2*).

all compounds ($S_2^{theor} \approx 6.9$—7.0 G^2). The experimental S_2 values of the NMR spectra in the 250—290 K region are somewhat higher (see Figs. 4 and 6). This implies that at temperatures below 290 K the F atoms occupy rather rigid positions in the crystalline lattice of the MSb_2F_7 compounds. The difference between S_2^{theor} and S_2^{exp} (~1.7—2.0 G^2) is associated with the anisotropy of the chemical shift, which is characteristic of the ^{19}F NMR spectra of alkali element fluoroantimonates(III).[3,14,15] Therefore, the observed asymmetry of the resonance line at temperatures below 290 K (see Fig. 5) should be related to both the structural nonequivalence of the F atoms in the lattice and anisotropy of CS. Note that the CS of the signals in the ^{19}F NMR spectra of compounds **1**—**3** at 290 K are arranged in the following sequence: 495 (**1**), 515 (**2**), and 485 ppm (**3**). Since the CS value is related to the nearest environment of the resonating nucleus, it is difficult to establish a certain correlation between the measured CS and the composition of the compounds due to the differences in structural arrangements of MSb_2F_7 (M = K, Rb, Cs), although many similarities are also observed. Therefore, the obtained δ values can be used only as some characteristics of these substances.

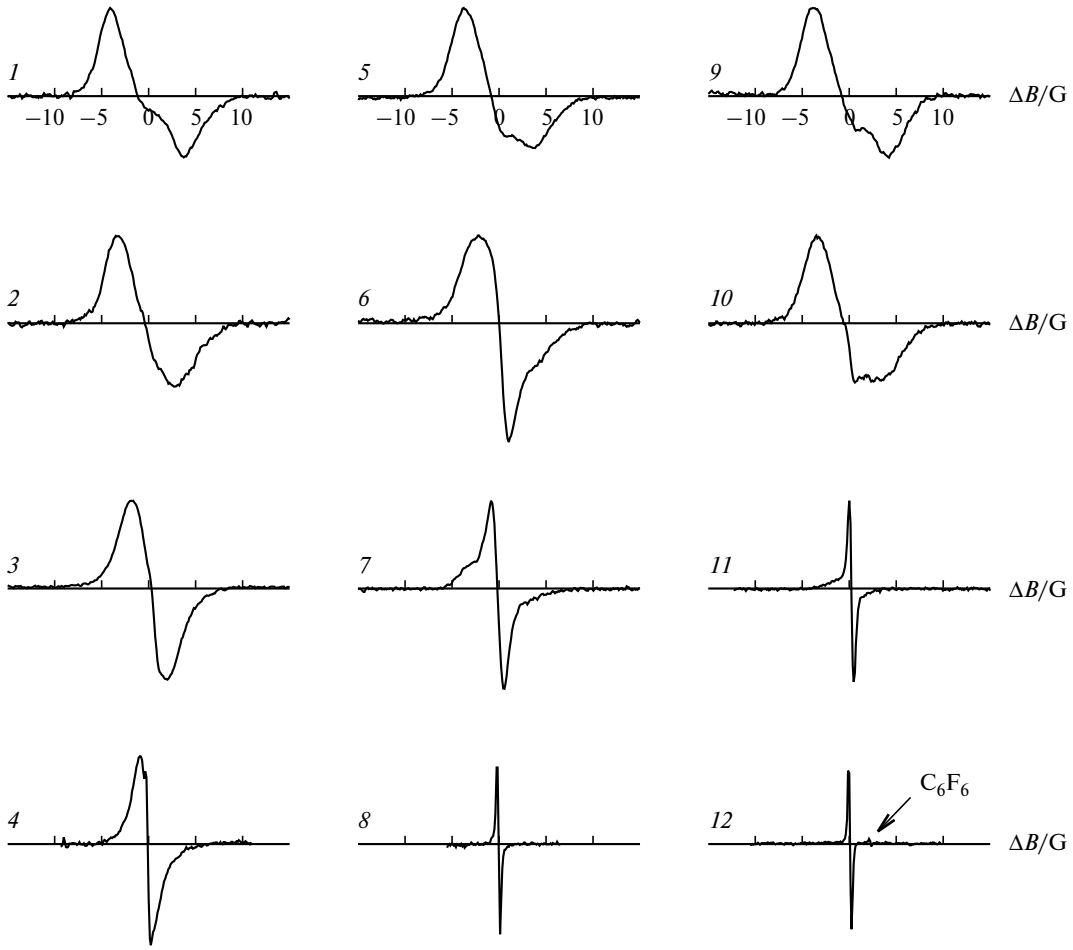

Fig. 5. ^{19}F NMR spectra of KSb_2F_7 (*1*—*4*), $RbSb_2F_7$ (*5*—*8*), and $CsSb_2F_7$ (*9*—*12*) at temperatures 280 (*1*, *5*, *9*), 320 (*6*), 350 (*2*, *7*), 365 (*10*), 390 (*3*), 420 (*11*), 455 (*12*), and 470 K (*4*, *8*).

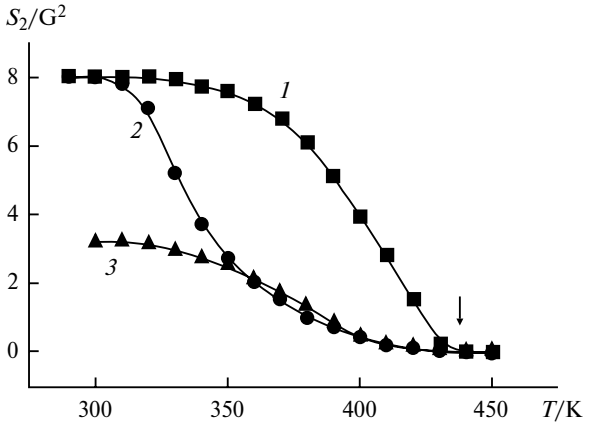

Fig. 6. Temperature plots of the second moment of the ^{19}F NMR spectra (S_2) of the $CsSb_2F_7$ compound (*1*) and its high-temperature modification β-$CsSb_2F_7$ (*2*, *3*): *2*, cooling and *3*, heating. The phase transition is shown by arrow.

Initial changes in the parameters of the ^{19}F NMR spectra of the compounds under study (transformation of the line shape, its narrowing, and a decrease in S_2) can be observed at 290 K and are attributed to the appearance of local motions in the fluorine subsystem. The lowest temperature needed for the development of this process (~290 K) is characteristic of compound **2** ($E_a \leq$ ≤ 46.0 kJ mol^{-1}), and compound **3** is characterized by the highest temperature (~350 K) ($E_a \approx 54.5$ kJ mol^{-1}). In compound **1** the local motions are activated ($E_a \approx$ 52.5 kJ mol^{-1}) at $T > 340$ K. The E_a value depends on the structure of compounds and strength of interionic interactions in them. The E_a values show that structure **2** possesses the most favorable conditions for the transition of the fluorine groups from the "rigid lattice" (in terms of NMR)[16] to local motions, while this transition is hindered, on the contrary, for structure **3**. Perhaps, this is caused by the fact that the dimers in structure **3** form layers linked by the Cs^+ cations that induce steric hindrances for the appearance of ion mobility (the nearest environment of the Cs^+ ions consists[9] of five F atoms at distances of 3.161—3.247 Å). Since the changes in the parameters of the ^{19}F NMR spectra at temperature variations differ for compounds **1**—**3**, is seems reasonable to consider the dynamics of their changes for each individual compound.

KSb_2F_7 sample. An increase in temperature to 350 K decreases the asymmetry of the resonance line (see Fig. 5, spectra *1* and *2*), and above 350 K the initial narrowing of the line in the NMR spectrum with a decrease in the S_2 value (see Fig. 4, curve *1*) can be observed. The spectrum consists of one signal, which becomes symmetric at 390—400 K (see Fig. 5, spectrum *4*), and its second moment remains almost unchanged on heating the sample from 400 to 440 K and equals ~3.2 G^2. The temperature increase to 470 K (maximum in experiment) only slightly decreases S_2, in this process $\Delta B \approx 1.2$ G at the modulation amplitude <0.45 G. This implies that diffusion processes are absent from the fluorine subsystem under these conditions, and the parameters of the ^{19}F NMR spectrum are determined by local motions of the fluorine groups.[19] It is these motions that partially eliminate nonequivalence of positions of the F atoms and anisotropy of CS. The absence of signals from the ^{123}Sb NQR spectra at $T > 300$ K is likely related to the same reason. It follows from the structure of compound **1** (see Fig. 1) that reorientations of the $Sb(1)EF_3$ and $Sb(2)EF_4$ groups around the F(7) and F(2) bridges is the most probable type of motion determining the line shape and the value of the second moment of the ^{19}F NMR line in the 350—440 K region. The detection of the single symmetric signal in the ^{19}F NMR spectra indicates the dynamic homogeneity of the fluorine subsystem and can imply the simultaneous onset of reorientation processes of various fluorine groups that proceed almost with one correlation frequency ν_c determined by the Arrhenius dependence.

$RbSb_2F_7$ sample. The transformations of the line shape in the ^{19}F NMR spectrum and its second moment for this compound occur at $T > 290$ K. In the 310—320 K region, a "narrow" line with increasing intensity is detected in the spectrum ($\Delta B \approx 2$ G, see Fig. 5, spectrum *6*). The intensity of the broad component decreases with heating of the substance. The resonance lines have different chemical shifts, resulting in a small asymmetry of the line shape in the NMR spectrum. The two-component character of the spectrum remains to ~440 K. The ΔB value of the "narrow" line decreases from ~2 G at 330 K to ~0.9 G at 380 K. In the 380—440 K temperature interval its value remains almost unchanged: 0.83±0.04 G (the second moment is ~0.7 G^2). At $T > 450$ K the ΔB and S_2 values decrease sharply. The NMR spectrum consists of almost one narrow line, whose second moment tends to zero, and its width at 470 K is determined by the modulation value, indicating the development of the diffusion motion in the fluorine subsystem ($E_a > 71.0$ kJ mol^{-1}). The latter can be induced by the polymorphous transformation in compound **2**. In fact, a diffuse peak, which can be attributed to the phase change, is observed at ~460 K in the differential curve of heating from 290 to 475 K. However, taking into account that this peak is situated near the melting point, we prefer to relate the changes in the NMR spectra at $T > 450$ K to the initial change in the aggregate state of the substance. As already mentioned above, the transformation of the parameters of the ^{19}F NMR spectra observed in the 320—440 K temperature interval is induced by local motions, including different reorientations of the fluorine groups of antimony. The presence of at least two components in the NMR spectrum points to the dynamic heterogeneity of the fluorine subsystem. Such a heterogeneity can be associated with both the structural

nonequivalence of resonating nuclei and scatter of the motion frequencies of the latter.[16,19]

$CsSb_2F_7$ sample. For this compound, the changes in the parameters of the ^{19}F NMR spectra (see Figs. 5 and 6) begin at $T > 350$ K and occur in a narrower temperature interval (~80°) compared to those observed for KSb_2F_7 (~130°) and $RbSb_2F_7$ (>150°). In a region of 350—400 K, the line shape is transformed (it becomes symmetric) simultaneously with a decrease in the second moment (see Fig. 6, curve *1*), which is related to the appearance of dynamic processes in the fluorine subsystem. Taking into account the structure of the compound, the reorientation of the Sb_2F_7 dimers around the F(1) bridging atom can be considered as the most appropriate model of motion in this temperature interval (see Fig. 1). A narrow component with the width comparable with the radio-frequency field modulation (0.5—0.7 G) appears in the NMR spectra in the 410—420 K interval. The integral intensity of this line increases rapidly, and that of the broad line decreases with a comparatively slight temperature increase. Both lines are fairly well described by Gauss curves, and the difference between their CS reaches ~15 ppm, indicating the structural nonequivalence of "highly mobile" and "stationary" F atoms and/or their groups. At $T > 425$ K the ^{19}F NMR spectrum consists of almost one narrow line, whose second moment tends to zero and the width ($\Delta B \leq 0.15$ G) is determined by apparatus characteristics. This unambiguously indicates the diffusion character of ions in the fluorine sublattice ($E_a < 65$ kJ mol^{-1}). Such a sharp change in the parameters of the NMR spectrum in a sufficiently narrow temperature interval is attributed, most probably, to the polymorphous transformation in the compound accompanied by the transition from the reorientation motion of the fluorine subsystem to the diffusion motion. In fact, according to the data of X-ray diffraction, NMR, and DTA studies, the structural phase transition in compound **3** occurs in the 425—430 K temperature region to form the high-temperature modification β-$CsSb_2F_7$. The differential curve of heating compound **3** at 425 K exhibits the *endo*-effect (in a helium flow, the latter was observed at 448 K),[13] which is assigned to the reversible phase transition. According to the NMR data, depending on the conditions of cooling β-$CsSb_2F_7$ from 450 to 290—300 K, the high-temperature modification can retain for some time (metastable state) or transform into the initial phase. In the case of a gradual temperature decrease, the pronounced hysteresis of the parameters of the NMR spectra (line shapes and S_2 values, see Fig. 6, curve *2*) is observed, indicating the possibility of overcooling the high-temperature phase when it transforms at $T < 320$ K into initial modification **3**. The β-$CsSb_2F_7$ phase does not transform into the initial modification on fast cooling to room temperature. This is unambiguously indicated by analysis of the X-ray diffraction patterns of the initial compound and its high-temperature modification, which were detected at 295 K (Table 2). Moreover, disordering of the β-$CsSb_2F_7$ phase is that the reorientation motions of the fluorine groups and their transition to the diffusion motion occur at lower temperatures than those in the initial modification (see Fig. 6, curve *3*).

Table 2. X-ray diffraction data for the $CsSb_2F_7$ compound and its high-temperature β-phase

d/Å	I (%)	d/Å	I (%)	d/Å	I (%)
$CsSb_2F_7$		$CsSb_2F_7$		β-$CsSb_2F_7$	
6.44	4	1.512	10	3.18	8
4.21	10	1.507	10	2.98	8
3.58	100	1.458	5	2.91	8
3.43	21	1.395	3	2.77	2
3.21	25	1.391	3	2.52	7
2.87	3	1.376	4	2.450	5
2.79	13	1.332	4	2.217	3
2.68	3	1.304	3	2.127	13
2.56	3	1.292	4	2.107	3
2.50	3			2.049	9
2.344	17	β-$CsSb_2F_7$		2.023	13
2.164	20	4.40	5	1.985	2
2.112	10	4.15	4	1.969	2
2.010	19	3.95	18	1.949	2
1.975	3	3.80	5	1.910	3
1.920	19	3.63	25	1.888	4
1.796	10	3.56	9	1.854	2
1.729	9	3.49	100	1.819	5
1.629	3	3.43	13	1.794	3
1.608	4	3.30	5	1.754	9
1.557	3	3.20	4		

Thus, the study of temperature changes in the parameters of the ^{123}Sb NQR (77—325 K) and ^{19}F NMR (240—470 K) spectra of the complex fluorides MSb_2F_7 (M = K, Rb, Cs) in combination with the X-ray diffraction and thermogravimetric data showed that the KSb_2F_7 and $RbSb_2F_7$ compounds, whose structures are built by nonequivalent antimony polyhedra have more rigid crystalline lattices than the $CsSb_2F_7$ crystals. The probability of the transition of the fluorine subsystem to the diffusion motion in MSb_2F_7 increases with an increase in the polarizability of the alkaline cation. A temperature increase results in the development of only reorientation motions in the fluorine subsystem of KSb_2F_7, whereas in $RbSb_2F_7$ diffusion processes are manifested only in the temperature region in which the aggregate state of the substance begins to change. Unlike these compounds, the crystal structure of $CsSb_2F_7$ with one type of antimony polyhedra is less resistant to temperature. In the 425—430 K interval, $CsSb_2F_7$ undergoes the structural phase transition accompanied by the appearance of the diffusion mobility in the fluorine subsystem and a high ion conductivity. According to the data of measurements of the ion conductivity (see Tables 3 and 4), on cooling the MSb_2F_7 samples (M = K, Rb, Cs) are characterized by a higher

Table 3. Characteristics of the ion conductivity of the MSb_2F_7 compounds obtained in the heating—cooling regime

Compound	ΔT/K	E_a/eV	$\log(A/\text{S K cm}^{-1})$
KSb_2F_7	300—415	0.037±0.002	−1.8±0.2
	425—453	1.34±0.02	13.9±0.2
	453—350	0.33±0.02	2.7±0.2
$RbSb_2F_7$	330—400	0.62±0.02	5.7±0.2
	400—453	1.16±0.02	12.4±0.2
	453—300	0.60±0.02	6.2±0.2
$CsSb_2F_7$	300—415	0.57±0.02	4.9±0.2
	415—453	1.24±0.02	12.8±0.2
	405—350	0.41±0.02	3.2±0.2

Table 4. Conductivities (σ) of the MSb_2F_7 compounds measured in the heating—cooling regime

Compound	T/K	σ/S cm^{-1}	Compound	T/K	σ/S cm^{-1}
KSb_2F_7	300	$1.4 \cdot 10^{-5}$	$RbSb_2F_7$	400	$1.0 \cdot 10^{-4}$
	405	$1.8 \cdot 10^{-5}$		435*	$4.0 \cdot 10^{-5}$
	453	$2.2 \cdot 10^{-4}$	$CsSb_2F_7$	350	$1.1 \cdot 10^{-6}$
	405	$1.0 \cdot 10^{-4}$		453	$1.7 \cdot 10^{-3}$
	440*	$5.3 \cdot 10^{-5}$		350	$5.0 \cdot 10^{-6}$
$RbSb_2F_7$	400	$2.3 \cdot 10^{-5}$		435*	$6.7 \cdot 10^{-5}$
	453	$7.2 \cdot 10^{-4}$			

* See Ref. 2.

ion conductivity than that on heating, *i.e.*, the hysteresis of σ takes place. For the α-phase of these compounds, the temperature dependence of the specific conductivity σ satisfies the Arrhenius—Frenkel equation: $\sigma T = A\exp(-E_a/kT)$ (A is the pre-exponential factor, and E_a is the activation energy of conductivity), and the experimental data are reproduced on heating to 415 K followed by cooling. Thus, in the MSb_2F_7 series (M = K, Rb, Cs) the ion conductivity increases with an increase in the ion radius of the alkaline metal (*i.e.*, with an increase in the polarizability of the ion) on heating to 453 K. Note that the sharp increase in the $\log(\sigma T)$ values observed for $RbSb_2F_7$ and KSb_2F_7 at $T > 420$—430 K is induced, most probable, by the phase change in these compounds to form high-temperature modifications. The favorable transferring properties in KSb_2F_7 in the absence of fast diffusion of the F^- ions can be caused, as in the case of Na_2SbF_5,[3] by the diffusion of the alkali cation.

This work was financially supported by the Russian Foundation for Basic Research (Project No. 02-03-32543).

References

1. L. M. Avkhutskii, R. L. Davidovich, L. A. Zemnukhova, P. S. Gordienko, V. Urbonavičius, and J. Grigas, *Phys. Stat. Sol. (b)*, 1983, **116**, 483.
2. M. P. Borzenkova, F. V. Kalinchenko, A. V. Novoselova, A. K. Ivanovits, and N. I. Sorokin, *Zh. Neorg. Khim.*, 1984, **29**, 703 [*J. Inorg. Chem. USSR*, 1984, **29** (Engl. Transl.)].
3. Yu. N. Moskvich, B. I. Cherkasov, A. M. Polyakov, A. A. Sukhovskii, and R. L. Davidovich, *Phys. Stat. Sol. (b)*, 1989, **156**, 615.
4. J. G. Bergman, D. S. Chemla, R. Fourcade, and G. Mascherpa, *J. Sol. Stat. Chem.*, 1978, **3**, 187.
5. E. A. Kravchenko, R. L. Davidovich, L. A. Zemnukhova, and Yu. A. Buslaev, *Dokl. Akad. Nauk SSSR*, 1974, **214**, 611 [*Dokl. Chem.*, 1974 (Engl. Transl.)].
6. T. Birchall and B. Della Valle, *Canad. J. Chem.*, 1971, **49**, 2808.
7. L. A. Zemnukhova and R. L. Davidovich, *Z. Naturforsch.*, 1998, **53a**, 573.
8. S. H. Mastin and R. R. Ryan, *Inorg. Chem.*, 1971, **10**, 1757.
9. R. R. Ryan, S. H. Mastin, and A. C. Larson, *Inorg. Chem.*, 1971, **10**, 2793.
10. D. Tichit, B. Ducourant, R. Fourcade, and G. Mascherpa, *J. Fluor. Chem.*, 1979, **13**, 45.
11. N. Habibi, B. Ducourant, R. Fourcade, and G. Mascherpa, *Bull. Soc. Chim. Fr.*, 1974, 2320.
12. Yu. Ya. Kharitonov, R. L. Davidovich, V. I. Kostin, L. A. Zemnukhova, and V. I. Sergienko, *Zh. Neorg. Khim.*, 1972, **27**, 1316 [*J. Inorg. Chem. USSR*, 1972, **27** (Engl. Transl.)].
13. R. L. Davidovich and L. A. Zemnukhova, *Koord. Khim.*, 1975, **1**, 477 [*Sov. J. Coord. Chem.*, 1975, **1** (Engl. Transl.)].
14. L. A. Zemnukhova, V. Ya. Kavun, G. A. Fedorishcheva, T. A. Kaidalova, and R. L. Davidovich, *Zh. Neorg. Khim.*, 1997, **42**, 1969 [*Russ. J. Inorg. Chem.*, 1997, **42** (Engl. Transl.)].
15. V. I. Sergienko, V. Ya. Kavun, and L. N. Ignat´eva, *Zh. Neorg. Khim.*, 1991, **36**, 3153 [*J. Inorg. Chem. USSR*, 1991, **36** (Engl. Transl.)].
16. A. G. Lundin and E. I. Fedin, *YaMR-spektroskopiya* [*NMR Spectroscopy*], Nauka, Moscow, 1986, 224 pp. (in Russian).
17. A. A. Udovenko and L. M. Volkova, *Koord. Khim.*, 1981, **7**, 1763 [*Sov. J. Coord. Chem.*, 1981, **7** (Engl. Transl.)].
18. H. Bayer, *Z. Physik*, 1951, **130**, 227.
19. S. P. Gabuda and A. G. Lundin, *Vnutrennyaya podvizhnost´ v tverdom tele* [*Internal Mobility in Solid State*], Nauka, Novosibirsk, 1986, 176 pp. (in Russian).

Received May 30, 2000;
in revised form March 21, 2001